Comparative study of the low-lying valence electronic states of carbon dioxide by high-resolution inelastic x-ray and electron scattering

Dong-Dong Ni,[1,2] Long-Quan Xu,[1,2] Ya-Wei Liu,[1,2] Ke Yang,[3,*] Nozomu Hiraoka,[4] Ku-Ding Tsuei,[4] and Lin-Fan Zhu[1,2,†]

[1]*Hefei National Laboratory for Physical Sciences at Microscale and Department of Modern Physics,*
University of Science and Technology of China, Hefei, Anhui 230026, People's Republic of China

[2]*Synergetic Innovation Center of Quantum Information and Quantum Physics, University of Science and Technology of China,*
Hefei, Anhui 230026, People's Republic of China

[3]*Shanghai Institute of Applied Physics, Chinese Academy of Sciences, Shanghai 201204, People's Republic of China*

[4]*National Synchrotron Radiation Research Center, Hsinchu 30076, Taiwan, Republic of China*

We report a comparative study of low-lying valence electronic states of carbon dioxide by high-resolution inelastic x-ray and electron scattering. Momentum-transfer-dependent inelastic squared form factors for the two states $^1\Sigma_u^+$ and $^1\Pi_u$ and generalized oscillator strength for the 9 eV feature from the ground state $X^1\Sigma_g^+$ have been derived from the inelastic x-ray scattering method at an impact photon energy around 10 keV, and the electron energy-loss spectra measured at an incident electron energy of 1500 eV. It is found from the comparison between the present results and the previous outcomes that the recent calculations taking the vibronic effects into consideration satisfactorily reproduce the inelastic squared form-factor profile for the $^1\Sigma_u^+$ transition and the generalized oscillator strength profile for the 9 eV feature. However, the vibronic effects seem to play no role in the $^1\Pi_u$ transition. The difference existing between the inelastic x-ray scattering and electron energy-loss spectroscopy results in the larger momentum-transfer squared region may be attributed to the increasing role of the higher-order Born terms. Furthermore, the controversy concerning the designations of electronic states around 11 eV is solved by assigning the two peaks centered at 10.98 and 11.05 eV to the vibrational progression $^1\Sigma_u^{+\prime}$ and $^1\Sigma_u^+$, and the peak centered at 11.16 eV to the forbidden transition $2^1\Delta_u$ based on the present results.

I. INTRODUCTION

Carbon dioxide is one of the fundamental constituents of the planetary atmosphere, especially in the Martian and Venusian atmospheres where it dominates. On Earth, its behavior is carefully scrutinized with respect to the global warming process. The molecule also plays an important role in laser technology, gaseous discharges, and low-temperature plasma devices. Furthermore, carbon dioxide is one of the simplest polyatomic molecules, thus its study is also of particular interest from the viewpoint of molecular spectroscopy [1–3]. For all of these practical and fundamental reasons, detailed information concerning the excitation processes of carbon dioxide has deservedly received considerable attention from the theorists and experimentalists alike.

Carbon dioxide has its own complexity over atoms and diatomic molecules in that the low-lying valence excited states prefer bent geometries, and it is likely that the changes in the electronic-state characters with the molecular geometry substantially affect the shapes of the associated spectral features, transition probabilities, and momentum-transfer-dependence behaviors [4]. However, most previous calculations for the $^1\Sigma_u^+$ and $^1\Pi_u$ transitions have been restricted to the ground-state nuclear conformation and the possible effects of molecular bending are neglected [4]. It was not until 2000 that Buenker *et al.* [4] obtained the theoretical results by means of multireference single- and double-excitation

configuration-interaction (MRD-CI) calculations and pointed out that the intense spectral features around 11 eV, being ascribed to the $^1\Sigma_u^+$ transition, are substantially influenced by the molecular bending. Using wave functions at the equation-of-motion coupled-cluster singles and doubles level, Watanabe *et al.* [2] have shown that taking into account vibronic effects by evaluating the electronic transition amplitudes along the individual normal coordinates results in satisfactory agreement between experiment and theory for the $^1\Pi_g$ and $^1\Delta_u$ transitions. Clearly, detailed knowledge of vibronic effects is needed to fully understand the electronic excitation processes of carbon dioxide. However, it is substantially difficult to determine the contribution of vibronic effects exclusively because there exists a great chance that the electron energy-loss spectroscopy (EELS) results contain the contribution of higher-order Born terms. Recent inelastic x-ray scattering (IXS) studies show that the higher-order Born terms also contributed considerably to the experimental differential cross section (DCS) in the electron-impact method, even at a high impact energy of several keV [5–8]. Previous measurements of generalized oscillator strength (GOS) of carbon dioxide [9,10] were conducted by the EELS method and it is very difficult to tell whether the first Born approximation (FBA) is reached based on their impact energies (200 eV [9], 300 eV [10], 500 eV [10], and 3000 eV [2]). The IXS method has the advantage over the EELS measurement in that the FBA is nearly always satisfied, thus it is suitable for the inelastic squared form factor (ISFF) by the IXS to serve as the high-energy limit of the electron-impact method. It will not only clarify the existing difference between theoretical calculations and preceding experiments, but also make it possible to evaluate the vibronic effects exclusively.

―――――――

*yangke@sinap.ac.cn

†lfzhu@ustc.edu.cn

The ISFF, or the equivalent physical quantity of the GOS, is one of the most important dynamic parameters since it is directly related to the electronic structure, i.e., the wave functions of the initial and final states, of atoms or molecules. Therefore, highly accurate experimental ISFFs or GOSs can be used to test the theoretical models and calculational codes rigorously [3,11–21]. It is commonly believed that the validity of converting the experimental DCS into the ISFF or GOS directly is guaranteed on the condition that the FBA is satisfied. The ISFF determined by the IXS or high-energy EELS is defined as

$$\zeta(\boldsymbol{q},\omega_n) = \left| \langle \Psi_n | \sum_{j=1}^{N} \exp(i\boldsymbol{q}\cdot\boldsymbol{r}_j) | \Psi_0 \rangle \right|^2, \qquad (1)$$

where $\boldsymbol{q}$ denotes the momentum transfer. Ψ_0 and Ψ_n stand for the wave functions of the initial and final states, respectively. The sum is over all electrons and $\boldsymbol{r}_j$ is the position vector of the jth electron. The ISFF can be determined from the DCSs measured by the IXS or high-energy EELS under the condition that the FBA is satisfied:

$$\begin{aligned} \zeta(\boldsymbol{q},\omega_n) &= \frac{1}{r_0^2} \frac{\omega_i}{\omega_f} \frac{1}{|\boldsymbol{\epsilon}_i\cdot\boldsymbol{\epsilon}_f^*|^2} \left(\frac{d\sigma}{d\Omega}\right)_\gamma \\ &= \frac{1}{4}\frac{k_i}{k_f} q^4 \left(\frac{d\sigma}{d\Omega}\right)_e \\ &= \frac{q^2}{2\omega_n} f(\boldsymbol{q},\omega_n). \end{aligned} \qquad (2)$$

$(\frac{d\sigma}{d\Omega})_\gamma$ and $(\frac{d\sigma}{d\Omega})_e$ represent the DCSs measured by the IXS and EELS; $f(\boldsymbol{q},\omega_n)$ symbolizes the GOS. The factor $|\boldsymbol{\epsilon}_i\cdot\boldsymbol{\epsilon}_f^*|^2$ is the product of the polarized directions of incident and scattered photons, and r_0 is the classical electron radius. ω_i, ω_f, and $\omega_n = \omega_i - \omega_f$ represent the energies of the incident photon, scattered photon, and the loss between them, respectively. k_i and k_f denote the momenta of the incident and scattered electrons.

The purpose of this study is to improve the knowledge of the low-lying electronic states of carbon dioxide. Emphases are primarily focused on the role of vibronic effects in reproducing the experimentally observed GOS and ISFF profiles and the existing difference between IXS and EELS results. The ISFFs of carbon dioxide have been measured over a wide momentum-transfer range using IXS and EELS methods. It has been shown from the comparisons between the experimental results and theoretical calculations that the vibronic effects play an important role in reproducing the experimentally observed ISFF profile of the $^1\Sigma_u^+$ transition and the GOS profile for the 9 eV feature, but it does not hold for the transition $^1\Pi_u$. Furthermore, we are also trying to resolve the controversy concerning the designations of electronic states around 11 eV.

II. EXPERIMENTAL METHOD

The present EELS experiment was conducted at the high-resolution electron energy-loss spectrometer, which has been described exhaustively in our previous works [22–25]. Thus we just give a concise description here. The apparatus is made of an electron gun, a hemispherical monochromator,

a rotatable energy analyzer, an interaction chamber, a series of cylindrical electrostatic optic lens, and a position-sensitive detector. All of these components are installed inside the corresponding vacuum chambers. The standard relative flow technique [25–27] was utilized to simplify the normalization processes and improve the accuracy of the experimental data. First, the mixed gases of carbon dioxide and helium with respectively controlled flowed rates flow into the interaction chamber simultaneously and continuously. Then intensity ratios of the excited states of carbon dioxide to those of helium are measured at an incident electron energy of 1500 eV with an energy resolution of 70 meV and angular range from 1.5° to 9°. Finally, it is possible with these ratios to determine the absolute inelastic DCSs of the carbon dioxide by normalizing them to the inelastic DCS of the 2^1P state of helium, which has been measured and calculated with high accuracy [28–31].

The IXS experiment was performed at the Taiwan beam line BL12XU at SPring-8 and the experimental procedures utilized are similar to those employed in our preceding works [5–7,31,32]. Accordingly, only a brief description will be given below. With the scattered photon energy fixed at 9889.43 eV, the energy loss was easily deduced by varying the incident photon energy gradually. The experiment was operated with an energy resolution around 70 meV. The excitation from the ground state to the 2^1P state of helium, whose GOS has been measured and calculated with high accuracy and proven to be credible [28–31], was measured at small scattering angles ($\leqslant 16°$) and utilized to normalize the results of carbon dioxide. In addition, in order to acquire the absolute value of $\zeta(\boldsymbol{q},\omega_n)$ for carbon dioxide, the pressures and the actual transmissivities of both carbon dioxide and helium were recorded to normalize the experimental data under the same experimental conditions.

III. RESULTS AND DISCUSSION

In order to obtain detailed information for the individual electronic states, a least-squares fitting is needed. However, the interpretation of the associated spectral features around 9 eV has remained controversial [2] and it is impossible to separate the 9 eV feature due to their large line widths. Therefore, we focus on the behavior concerning the 9 eV feature in this paper and it is constructed by a sum of two Gaussian functions centered at 8.4 and 9.3 eV, which correspond to $^1\Delta_u$ and $^1\Pi_g$, as illustrated in Fig. 1(a). The least-squares fitting around 11.05 and 11.40 eV is extremely complicated, as shown in Figs. 1(b) and 1(c), and a brief instruction is given below. First, there is no doubt that the peak centered at 11.40 eV is the state $^1\Pi_u$ [2,9,10,33]. Then, we assign the two peaks centered at 10.98 and 11.05 eV to the vibrational progressions $^1\Sigma_u^{+'}$ and $^1\Sigma_u^+$, and the peak centered at 11.16 eV to the forbidden transition $2^1\Delta_u$ based on the present experimental results and our careful analysis, which will be discussed in detail below. Furthermore, the two peaks at 11.10 and 11.21 eV stand for $^{1,3}\Delta_u$ and $^3\Sigma_u^-$, respectively, according to Ref. [9]. In addition to the above-mentioned peaks, the remaining peaks, centered at 10.72, 10.80, 10.86, 10.92, 11.29, 11.34, and 11.45 eV, are added to achieve the best-fit results according to Ref. [9]. Given the fact that the 11.05 and 11.40 eV transitions are considered as a single peak in the previous lower-resolution EELS experiments [2,10], the sum of the
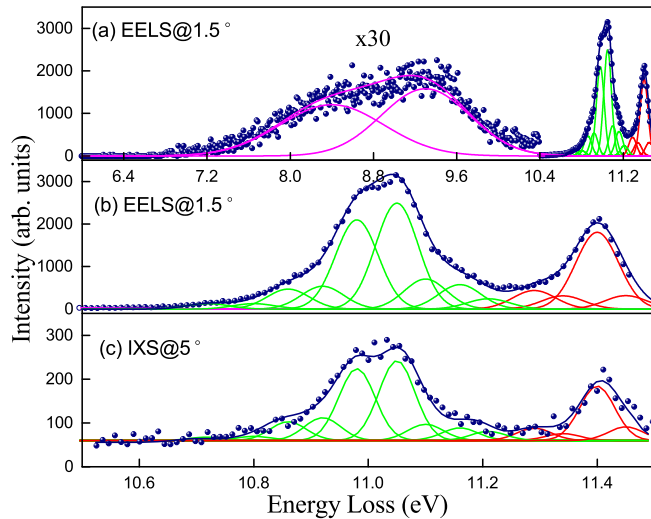
FIG. 1. Present EELS and IXS spectra of carbon dioxide and the corresponding fitted results. The 9 eV feature in (a) has been multiplied by a factor of 30. The energy axis in (b) is the same as that in (c).

green peaks and the aggregate of the red peaks as displayed explicitly in Figs. 1(b) and 1(c) are presented for the purpose of comparison. The statistics of counts, the fitting procedure, and the normalizing process contribute mainly to the errors of the two experiments above, and the experimental errors are shown in the corresponding figures.

Figure 2 shows the GOS for the 9 eV feature, which includes the transitions from the ground state $X\,^1\Sigma_g^+$ to $^1\Pi_g$, $^1\Sigma_u^-$, and $^1\Delta_u$. It should be emphasized here that the three transitions are all dipole forbidden in the linear nuclear arrangement [34]. However, they become allowed in the frame of bending
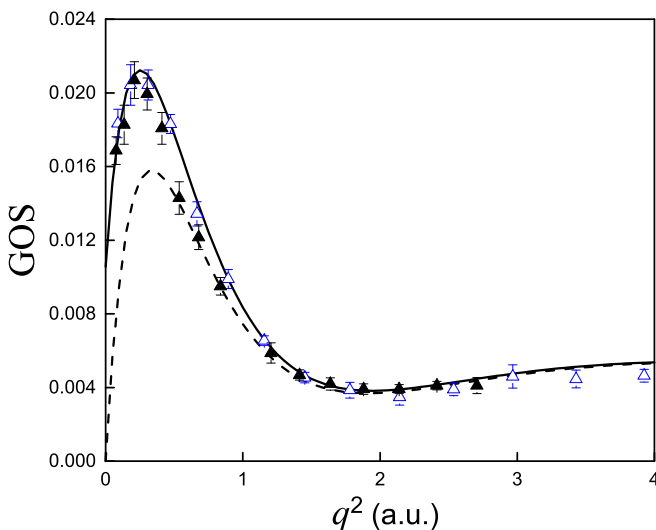
FIG. 2. The GOS for the 9 eV feature. The solid black triangles and the open blue triangles stand for the EELS results at impact electron energies of 1500 and 3000 eV [2], respectively. The black solid line and dashed line are the theoretical calculations by Watanabe *et al.* [2] and the difference lies in that the former takes the vibronic effects into consideration.
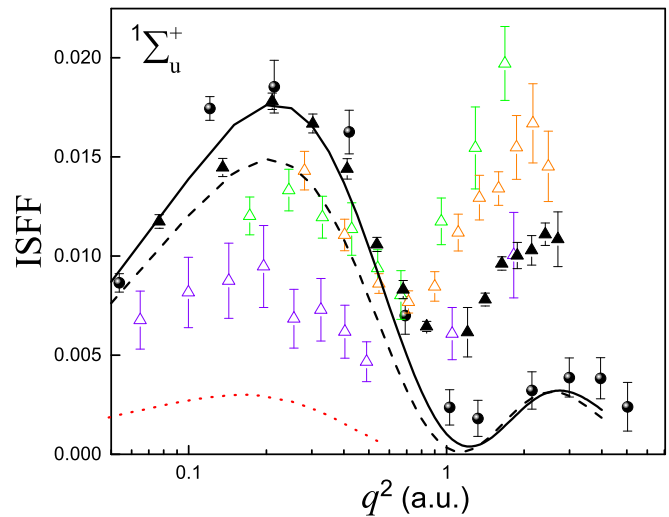
FIG. 3. The ISFF for the excitation to $^1\Sigma_u^+$. The solid black circles and solid black triangles stand for the present IXS and EELS results, respectively. The preceding EELS results are 200 eV (open violet triangles) [9], 300 eV (open green triangles) [10], and 500 eV (open orange triangles) [10]. The red dotted line represents the theoretical calculation by Buenker *et al.* [4]. The black solid line and dashed line are the theoretical calculations by Watanabe *et al.* [2] and the difference lies in that the former takes vibronic effects into account.

structure and acquire relatively weak intensity at the optical limit of $q^2 \rightarrow 0$. Given the fact that the ground state is in the linear equilibrium geometry, the momentum-dependent behavior of the 9 eV feature in the form of the GOS is consistent with that of a forbidden transition which has the characteristic that its GOS first increases with the momentum transfer, then reaches the maximum, and decreases gradually thereafter. It is clear in Fig. 2 that there exists excellent agreement between the preceding EELS results [2] at an impact electron energy of 3000 eV and the present EELS one at an impact electron energy of 1500 eV over the whole range, suggesting that the FBA is satisfied and the contribution of higher-order Born terms can be neglected. Furthermore, the theoretical calculations taking the vibronic effects into consideration satisfactorily reproduce the EELS results, and the findings demonstrate that taking the vibronic effects into account is essential for a proper understanding of the nature of the transitions.

The present ISFFs for the transition to $^1\Sigma_u^+$ are presented in Fig. 3 along with the previous EELS results [9,10] and theoretical calculations [2,4]. In contrast to the present IXS and EELS results, the calculated result by Buenker *et al.* [4] is about a factor of 3 smaller. The substantial deviation from experiments is, at least partly, due to the limited size of the basis set used [2], and Buenker *et al.* [4] have, in fact, shown that using a larger basis set considerably reduces the discrepancy. The significant role of the vibronic effects is manifested through the comparison between the calculation by taking the equilibrium geometry and the one by taking the vibronic effects into consideration. It is obvious that the theoretical calculation by Watanabe *et al.* [2] taking the vibronic effects into account satisfactorily reproduces the present IXS results, and the excellent accordance over the whole momentum-transfer squared region strongly suggests
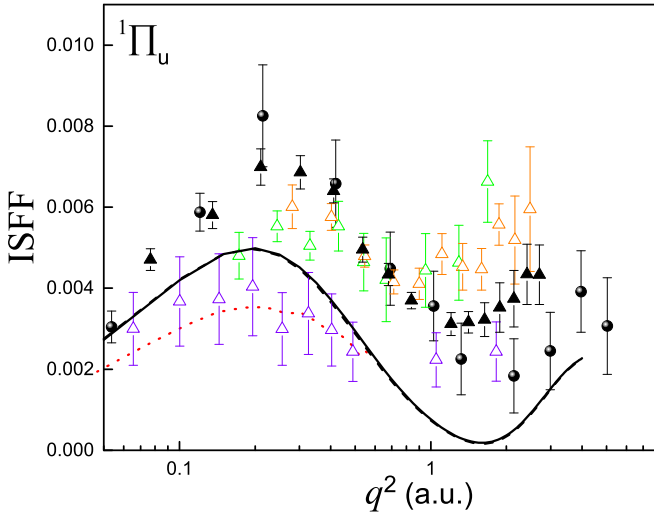
FIG. 4. Same as Fig. 3, but for $^1\Pi_u$ centered at 11.40 eV. The black solid line and dashed line almost coincide over the whole momentum-transfer squared region.

FIG. 5. The present EELS spectra at different angles. The black, red, green, and navy solid lines stand for the spectra taken at $2°$, $4°$, $6°$, and $8°$, respectively. The results of $4°$, $6°$, and $8°$ have been normalized to the spectrum of $2°$ at 11.05 eV for the purpose of comparison. In order to see the trend more clearly, the 9 eV feature has been multiplied by a factor of 3.

that the present IXS result serves as the benchmark data for the $^1\Sigma_u^+$ transition. While the present EELS results at electron-impact energy of 1500 eV agree well with the IXS outcomes in the region $q^2 < 1$ a.u., the preceding EELS results at electron-impact energies of 200 eV [9], 300 eV [10], and 500 eV [10] are still remarkably lower than the present IXS ones in this q^2 region. This phenomenon demonstrates that the FBA is satisfied at an impact energy of 1500 eV in the region of $q^2 < 1$ a.u., but it does not hold at electron-impact energies of 200 eV [9], 300 eV [10], and 500 eV [10]. In the region of $q^2 > 1$ a.u. where the vibronic effects can be neglected, there is an obvious tendency that the deviations between the EELS and IXS decrease with the increase of the electron-impact energy. However, the EELS result at impact energy of 1500 eV is still larger than the IXS one in magnitude even with the error bar, which may be attributed to the increasing role of higher Born terms in the larger momentum transfer. It should be emphasized that the EELS result at electron-impact energy of 200 eV [9] only takes the contributions of the peaks centered at 10.98 and 11.05 eV, which may account for the occasional coincidence of the EELS results at electron-impact energies of 1500 and 200 eV in $q^2 > 1$ a.u.

Figure 4 shows the ISFFs of $^1\Pi_u$ determined in the present works along with the theoretical calculations [2,4] and EELS values [9,10] converted from the reported GOSs. The discrepancy between the MRD-CI calculation by Buenker *et al.* and the present results gets smaller for the state $^1\Pi_u$ than that for the $^1\Sigma_u^+$ transition, which may be due to the fact that the $^1\Pi_u$ transition is less sensitive to the theoretical treatment of the wave functions than for the $^1\Sigma_u^+$ transition. It seems that there is no appreciable difference between the equilibrium geometry and vibronic effects calculations by Watanabe *et al.* [2]. Although the theoretical calculations seem to slightly underestimate the presently measured IXS and EELS results over the whole momentum-transfer squared region, the overall shapes are in reasonably good agreement with each other. The good agreement between the IXS results and the EELS outcomes at impact-electron energy of 1500 eV

in the region $0 < q^2 < 1$ a.u. indicates that the FBA is satisfied in this region. Though the difference between the IXS results and EELS outcomes seems to decrease with respect to the increase of the impact-electron energy in the region of $q^2 > 1$ a.u., the EELS results are still larger in magnitude than the IXS one on the whole, which may be due to the breakdown of the FBA even at an electron energy of 1500 eV.

It has always been controversial to assign the states around 11 eV. While Franksin *et al.* [33] considered the peaks centered at 10.98 and 11.05 eV being members of a vibrational progression $^1\Sigma_u^{+\prime}$ and $^1\Sigma_u^+$, Buenker *et al.* [4] held the view that they belong to the distinct singlet electronic states of classification $^1\Delta_u$ and $^1\Sigma_u^+$. It has been displayed by Green *et al.* [9] that the ratio of the peak intensity centered at 11.05 eV to that at 10.98 eV remains constant with respect to the scattering angle, which strongly suggests that the two peaks belong to the two vibrational progressions of the same electronic state. In spite of the fact mentioned above, they still tend to agree with the viewpoint of Buenker *et al.* [4]. Furthermore, the recent calculation by Watanabe [2] revealed that there were three states around 11 eV, namely, $^1\Sigma_u^+$ (11.08 eV), $2^1\Delta_u$ (11.16 eV), and $2^1\Sigma_u^-$ (11.21 eV), and the intensity of $2^1\Sigma_u^-$ is much less than that of $2^1\Delta_u$. So the transition of $2^1\Sigma_u^-$ is neglected in the following discussion. According to the selection rule in the linear nuclear arrangement, the former is dipole allowed and the latter two are strictly dipole forbidden [34]. However, the $2^1\Delta_u$ transition becomes allowed in the frame of bending geometry and it should be weak in the small-q^2 region. It is shown clearly in Fig. 5(b) that in addition to the two peaks centered at 10.98 and 11.05 eV, there exists another peak centered around 11.16 eV, whose intensity with respect to the scattering angle shares the same trend with that of the 9 eV feature ($^1\Pi_g$, $^1\Sigma_u^-$, and $^1\Delta_u$), as suggested in Fig. 5(a). In addition, the corresponding peak intensity centered at 11.16 eV scales proportionally to

the scattering angle (momentum transfer), then reaches its maximum, and decreases gradually at last, which is a typical characteristic of a forbidden transition. We conclude with confidence that the two peaks centered at 10.98 and 11.05 eV are the vibrational progressions $^1\Sigma_u^{+\prime}$ and $^1\Sigma_u^+$, and the peak centered at 11.16 eV belongs to the forbidden transition $2^1\Delta_u$.

IV. SUMMARY AND CONCLUSION

In this study, the GOSs and ISFFs of low-lying valence electronic states of carbon dioxide were determined based on the high-resolution IXS and EELS methods. By comparing the present experimental results with the preceding EELS outcomes and theoretical calculations, some meaningful conclusions have been reached. The vibronic effects play an important role in reproducing the ISFF profile of $^1\Sigma_u^+$ and the GOS profile of the 9 eV feature, while its contribution is negligible for the transition $^1\Pi_u$. The FBA is satisfied

for transitions $^1\Sigma_u^+$ and $^1\Pi_u$ at an impact-electron energy of 1500 eV when $0 < q^2 < 1$ a.u., but it does not hold in the region of $q^2 > 1$ a.u. In addition, we assign the two peaks centered at 10.98 and 11.05 eV to the vibrational progression $^1\Sigma_u^{+\prime}$ and $^1\Sigma_u^+$, and the peak centered at 11.16 eV to the forbidden transition $2^1\Delta_u$ based on our EELS results.

[1] Y. Itikawa, J. Phys. Chem. Ref. Data **31**, 749 (2002).

[2] N. Watanabe, T. Hirayama, D. Suzuki, and M. Takahashi, J. Chem. Phys. **138**, 184311 (2013).

[3] J. Inkinen, A. Sakko, K. O. Ruotsalainen, T. Pylkkänen, J. Niskanen, S. Galambosi, M. Hakala, G. Monaco, S. Huotari, and K. Hämäläinen, Phys. Chem. Chem. Phys. **15**, 9231 (2013).

[4] R. J. Buenker, M. H. Honigmann, H. P. Liebermann, and M. Kimura, J. Chem. Phys. **113**, 1046 (2000).

[5] L. F. Zhu, W. Q. Xu, K. Yang, Z. Jiang, X. Kang, B. P. Xie, D. L. Feng, N. Hiraoka, and K. D. Tsuei, Phys. Rev. A **85**, 030501(R) (2012).

[6] X. Kang, K. Yang, Y. W. Liu, W. Q. Xu, N. Hiraoka, K. D. Tsuei, P. F. Zhang, and L. F. Zhu, Phys. Rev. A **86**, 022509 (2012).

[7] Y. G. Peng, X. Kang, K. Yang, X. L. Zhao, Y. W. Liu, X. X. Mei, W. Q. Xu, N. Hiraoka, K. D. Tsuei, and L. F. Zhu, Phys. Rev. A **89**, 032512 (2014).

[8] J. A. Bradley, G. T. Seidler, G. Cooper, M. Vos, A. P. Hitchcock, A. P. Sorini, C. Schlimmer, and K. P. Nagle, Phys. Rev. Lett. **105**, 053202 (2010).

[9] M. A. Green, P. J. O. Teubner, L. Campbell, M. J. Brunger, M. Hoshino, T. Ishikawa, M. Kitajima, H. Tanka, Y. Itikawa, M. Kimura *et al.*, J. Phys. B: At. Mol. Opt. Phys. **35**, 567 (2002).

[10] K. N. Klump and E. N. Lassettre, J. Electron. Spectrosc. Relat. Phenom. **14**, 215 (1978).

[11] Z. Chen, A. Z. Msezane, and M. Y. Amusia, Phys. Rev. A **60**, 5115 (1999).

[12] M. Y. Amusia, L. V. Chernysheva, Z. Felfli, and A. Z. Msezane, Phys. Rev. A **65**, 062705 (2002).

[13] M. Vos, R. P. McEachran, G. Cooper, and A. P. Hitchcock, Phys. Rev. A **83**, 022707 (2011).

[14] A. N. Hopersky, A. M. Nadolinsky, K. K. Ikoeva, and O. A. Khoroshavina, J. Exp. Theor. Phys. **113**, 731 (2011).

[15] A. N. Hopersky, A. M. Nadolinsky, K. K. Ikoeva, and O. A. Khoroshavina, J. Phys. B: At. Mol. Opt. Phys. **44**, 145202 (2011).

[16] J. Lehtola, V. Hakala, and K. Hämäläinen, Phys. Chem. Chem. Phys. **13**, 5630 (2011).

[17] J. A. Bradley, A. Sakko, G. T. Seidler, A. Rubio, M. Hakala, K. Hämäläinen, G. Cooper, A. P. Hitchcock, K. Schlimmer, and K. P. Nagle, Phys. Rev. A **84**, 022510 (2011).

[18] A. Sakko, A. Rubio, M. Hakala, and K. Hämäläinen, J. Chem. Phys. **133**, 174111 (2010).

[19] J. Inkinen, J. Niskanen, A. Sakko, K. O. Ruotsalainen, T. Pylkkänen, S. Galambosi, M. Hakala, G. Monaco, K. Hämäläinen, and S. Huotari, J. Phys. Chem. A **118**, 3288 (2014).

[20] A. M. Carrascosa, T. Northey, and A. Kirrander, Phys. Chem. Chem. Phys. **19**, 7853 (2017).

[21] N. Thomas, A. M. Carrascosa, S. Schäfer, and A. Kirrander, J. Chem. Phys. **145**, 154304 (2016).

[22] S. L. Wu, Z. P. Zhong, R. F. Feng, S. L. Xing, B. X. Yang, and K. Z. Xu, Phys. Rev. A **51**, 4494 (1995).

[23] K. Z. Xu, R. F. Feng, S. L. Wu, Q. Ji, X. J. Zhang, Z. P. Zhong, and Y. Zheng, Phys. Rev. A **53**, 3081 (1996).

[24] X. J. Liu, L. F. Zhu, X. M. Jiang, Z. S. Yuan, B. Cai, X. J. Chen, and K. Z. Xu, Rev. Sci. Instrum. **72**, 3357 (2001).

[25] Y. W. Liu, L. Q. Xu, D. D. Ni, X. Xu, X. C. Huang, and L. F. Zhu, J. Geophys. Res. Space Phys. **122**, 3459 (2017).

[26] M. A. Khakoo and S. Trajmar, Phys. Rev. A **34**, 138 (1986).

[27] J. C. Nickel, P. W. Zetner, G. Shen, and S. Trajmar, J. Phys. E: Sci. Instrum. **22**, 730 (1989).

[28] N. M. Cann and A. J. Thakkar, J. Electron. Spectroc. Relat. Phenom. **123**, 143 (2002).

[29] X. J. Liu, L. F. Zhu, Z. S. Yuan, W. B. Li, H. D. Cheng, J. M. Sun, and K. Z. Xu, J. Electron. Spectroc. Relat. Phenom. **135**, 15 (2004).

[30] X. Y. Han and J. M. Li, Phys. Rev. A **74**, 062711 (2006).

[31] B. P. Xie, L. F. Zhu, K. Yang, B. Zhou, N. Hiraoka, Y. Q. Cai, Y. Yao, C. Q. Wu, E. L. Wang, and D. L. Feng, Phys. Rev. A **82**, 032501 (2010).

[32] L. F. Zhu, L. S. Wang, B. P. Xie, K. Yang, N. Hiraoka, Y. Q. Cai, and D. L. Feng, J. Phys. B **44**, 025203 (2011).

[33] M. J. Hubin-Franskin, J. Delwiche, and D. Roy, J. Phys. B **21**, 3211 (1988).

[34] L. F. Zhu, H. C. Tian, Y. W. Liu, X. Kang, and G. X. Liu, Chin. Phys. B **24**, 043101 (2015).